

# Unstable Dynamical Properties of Spiral Cloud Bands in Tropical Cyclones\*

HUANG Hong<sup>1,2†</sup>(黄泓) and ZHANG Ming<sup>1</sup>(张铭)

<sup>1</sup> Institute of Meteorology, PLA University of Science and Technology, Nanjing 211101

<sup>2</sup> Shanghai Typhoon Institute, China Meteorological Administration, Shanghai 200030

(Received October 28, 2008)

## ABSTRACT

A nondivergent barotropic model (Model 1) and a barotropic primitive equation vortex model (Model 2) are linearized respectively in this paper. Then their perturbation wave spectrums are computed with a normal mode approach to study the instability problem on an appointed tropical cyclone (TC)-like vortex, thereby, the dynamic instability properties of spiral cloud bands of TCs are discussed.

The results show that the unstable mode of both models exhibits a spiral band-like structure that propagates away from the vortex outside the radius of maximum winds. The discrete modal instability of the pure vortex Rossby wave can account for the generation of the eyewall and the inner spiral band. The unstable mode in Model 2 has three parts, i.e., eyewall, inner and outer spiral bands. This mode can be interpreted as a mixed vortex Rossby-inertia gravitational wave. The unbalanced property of the wave outside the stagnation radius of the vortex Rossby wave is one of the important reasons for the formation of the outer spiral band in TCs. Accordingly, the outer spiral band can be identified to possess properties of an inertial-gravitational wave.

When the formation of unstable inner and outer spiral bands is studied, a barotropic vortex model shall be used. In this model, the most unstable perturbation bears the attributes of either the vortex Rossby wave or the inertial-gravitational wave, depending on the vortex radius. So such perturbations shall be viewed as an unbalanced and unstable mixed wave of these two kinds of waves.

**Key words:** tropical cyclone, spiral cloud bands, unbalanced instability, mixed vortex Rossby-inertia gravitational wave

**Citation:** Huang Hong and Zhang Ming, 2009: Unstable dynamical properties of spiral cloud bands in tropical cyclones. *Acta Meteor. Sinica*, **23**(4), 485–493.

## 1. Introduction

Tropical cyclones (TCs) are intense atmospheric vortices that develop over the warm tropical oceans. They are among the most feared and deadly weather systems on the earth. Accurate forecasting of both the track and intensity of a TC is critical to mitigating disasters potentially caused by an approaching TC. Successful forecasting of the track and intensity of TCs remains one of the most difficult and exciting challenges in meteorology. Forecasts of the TC motion have improved steadily over the last few decades (Xu, 1999; McAdie and Lawrence, 2000; Chen, 2001). In contrast, there has been relatively little advance in prediction of the TC intensity and its change (Avila, 1998; DeMaria and Kaplan, 1999; Duan et al., 2005). Among

many reasons (such as inadequate observations over the ocean, inadequate model resolution and physics, and poor initial conditions), deficient understanding of the dynamical property of the TC including its spiral cloud (rain) bands is a fundamental one. Spiral bands, which play an important role in the changes of path and intensity of TCs, are among the most important asymmetric features of the TC (Liu and Yang, 1980). So the study on their dynamical property constitutes an important part in the overall research on TCs.

Spiral bands were found firstly after the World War II (Maynard, 1945; Wexler, 1947). The banded structure of hurricanes and typhoons has been noted in many observational studies where radar or aircraft data were available. It is suggested by a lot of analyses

\*Supported by the Typhoon Research Fund of Shanghai Typhoon Institute, China Meteorological Administration, under Grant No. 2008ST06, and the National Natural Science Foundation of China under Grant No. 40575023.

<sup>†</sup>Corresponding author: hhong7782@163.com.

that spiral bands are a manifestation of the inertia-gravity wave (Abdullah, 1966; Liu, 1981). The occurrence, intensification, and decay of spiral bands in TCs were ever investigated by Zhang and Zeng (1983) using a five-level primitive equation quasi-spectrum model. They suggested that the property of spiral bands at the mature stage of a TC is very complicated and different from the typical inertial-gravity wave. The wave action conservation and the wave evolution in a TC-scale vortex were also studied with the WKBJ (Wentzel-Kramers-Brillouin-Jeffreys) approach (Huang and Chao, 1980; Chen, 1984).

Spiral bands can be conveniently divided into two classes: inner bands and outer bands (Guinn and Schubert, 1993). Inner bands lie close to the vortex center and, while evident on radar images, are often invisible on satellite images because of the cirrus overcast. Inner bands can form through generation of vortex Rossby waves, vortex merger, and diabatic sources away from the cyclone center. Outer bands are typically located more than 500 km from the vortex center and can be quite long and narrow. They form as a result of the nonlinear effects during the breakdown of the intertropical convergence zone (ITCZ) through barotropic instability.

TCs are localized vortices with elevated cyclonic potential vorticity (PV) concentrated in the inner core region near the radius of maximum wind (RMW) with large radial gradients. Any radial perturbation of air parcel would experience restoring force due to the presence of PV gradients, and generate edge PV waves. Because of their resemblance to the Rossby waves in the mid-latitude large-scale motion (Yu, 2002), these PV waves are usually termed as vortex Rossby waves (VRWs), i.e., Rossby-type waves in a circular vortex. This concept was originally proposed by MacDonald (1968).

Building on earlier work, which had identified vortex axisymmetrization as a universal process of smoothly distributed perturbed vortices (Guinn and Schubert, 1993), Montgomery and Kallenbach (1997) developed a theoretical framework on the VRW-guide model of vortex axisymmetrization. They suggested that the radially outward-propagating VRWs are re-

sponsible for initiation of the inner spiral rainband, and can affect the structure and intensity of the mean vortex by wave-mean flow interaction.

However, the outer rainband (outside a radius of about 80 km from the TC center) could not be explained by VRWs where the radial PV gradients become too weak. Chow et al. (2002) showed that fluctuations of the PV distribution in the TC core region can act as a source, generating gravity waves that produce banded structures and the moving spiral rainbands. Such fluctuations or rotation of the inner core PV distribution can result from the activity of VRWs in the TC eyewall (Wang, 2002a, b).

In his numerical simulations, Wang (2001, 2002a, b) showed that the outer spiral rainband most frequently forms and develops between 80 and 150 km from the TC center. There are several possible explanations for this preference. One explanation lies in the effect of downdrafts from anvil clouds in the outflow layer (Willoughby et al., 1984). The location of the outer spiral rainband is thus mainly determined by the outflow radial wind speed and the terminal velocity of ice species (snow and graupel) in the upper part of the eyewall. This may occur at a radius of about 100 km for strong TCs, consistent with the model results. Another mechanism is that proposed by Montgomery and Kallenbach (1997), who suggested that the outer spiral rainband could form near the stagnation radius of the VRWs at which the outward group velocity of the VRWs vanishes. Since both mechanisms coexist, further studies are needed to assess which mechanism is dominant in generating the outer spiral rainband.

The linearization was proven to be a good way to describe some hurricane characteristics at the mature stage, and it remains to be the preferred method until now (Chanh, 2004). The wave spectrum of perturbation can be computed by a norm mode approach. Then the evolution of unstable perturbations can be studied (Zeng, 1990, 1991). Instability problem can also be studied with the WKBJ approach, however, it is more suitable to explain the perturbation evolution in a heterogeneous medium (Chen, 1984). Furthermore, it is only applicable for a slow manifold, which is difficult to be

judged and is always dependent on experience. So linearization theory is adopted in this paper.

We now give an outline of the main text. TCs are baroclinic in nature, but the basic flow of strong TCs can be regarded as circular symmetric. As a crude approximation, TCs at lower levels can be seen as barotropic vortices (Zhang, 1995), so two barotropic vortex models will be presented in Section 2. The concept that the inner spiral rain band is closely associated with VRWs has been accepted widely, so a non-divergent barotropic vortex model (referred to as Model 1 for short) will be studied at first, which filters acoustic and inertia-gravitational waves and can describe the important property of unstable VRWs. Based on this model, a barotropic primitive equation vortex model (referred to as Model 2) will be used in order to give an insight into the dynamical instability properties of inner and outer spiral bands in a TC-like vortex. An empirical expression will be used to define a symmetric vortex as the basic-state flow in Section 3. Using the appointed basic state profile and vortex models, in Section 4, we will compute the eigenvalues and eigenvectors of the coefficient matrix for each wavenumber considered and find the most unstable mode. Then, the structure and dynamical properties of this unstable perturbation will be investigated. Conclusions will be presented in Section 5.

## 2. Description of barotropic vortex models

### 2.1 The non-divergent barotropic vortex model

Because observations show small deviations from circular symmetry in the near-core region of hurricanes (Shapiro and Montgomery, 1993), a useful zeroth-order approximation may be applied to studies of the linearized dynamics of a circular vortex in gradient balance. Linearization can be adopted to separate the balanced mean field from the total field. Then the linearized perturbation equation can be studied. The prototype model is that of a two-dimensional non-divergent inviscid flow on an  $f$ -plane, which has been used commonly in the research on VRWs in TCs. In a stationary cylindrical coordinate system, the lin-

earized vorticity equation is

$$\frac{\partial \zeta}{\partial t} = \frac{1}{r} \frac{d\bar{\eta}}{dr} \frac{\partial \psi}{\partial \lambda} - \bar{\Omega} \frac{\partial \zeta}{\partial \lambda}, \quad (1)$$

where

$$\zeta = \nabla^2 \psi = \frac{1}{r} \frac{\partial}{\partial r} \left( r \frac{\partial \psi}{\partial r} \right) + \frac{1}{r^2} \frac{\partial^2 \psi}{\partial \lambda^2}. \quad (2)$$

Here,  $r$  and  $\lambda$  denote the radial and azimuthal coordinates respectively;  $\psi$  is perturbation stream function;  $\zeta = \nabla^2 \psi$  is perturbation vorticity;  $\bar{V}(r)$  is the basic-state tangential wind;  $\bar{\eta} = f + d(r\bar{V})/(rdr)$  is the basic-state absolute vorticity;  $f$  denotes a constant Coriolis parameter (i.e.,  $0.5 \times 10^{-4} \text{s}^{-1}$ ); and  $\bar{\Omega} = \bar{V}/r$  is mean angular velocity. The basic-state  $\bar{V}$  satisfies the gradient wind balance

$$f\bar{V} + \frac{\bar{V}^2}{r} = \frac{d\bar{\phi}}{dr}. \quad (3)$$

The boundary condition of this model is set as

$$\psi = 0, r = 0; \quad \psi = 0, r = \tilde{r}, \quad (4)$$

where  $\tilde{r}$  denotes the maximum radius of a vortex, i.e., the outer boundary of the vortex;  $\bar{\Omega}$  is the function of  $r$ . The analytical solutions are difficult to obtain even for such a simple vortex model as Eq. (1). Therefore, we transform the initial value problem into an eigenvalue problem through introducing a norm mode. Then the equation is discretized and solved numerically. In this way, its spectrum points and functions can be obtained and analyzed.

The solution to Eq. (1) can be represented as

$$\psi = \Psi(r)e^{i(n\lambda - \sigma t)}, \quad (5)$$

where  $n$  denotes the azimuthal wavenumber and  $\sigma$  the wave frequency, i.e., wave spectrum. Substitute Eq. (5) into Eq. (1) and discretize this equation with corresponding boundary condition

$$\Psi_1 = 0, \quad \Psi_{N+1} = 0. \quad (6)$$

Here, subscript 1 denotes the vortex center, and  $N+1$  the outer boundary of the vortex. Then the discrete system yields a standard matrix-eigenvalue problem,

$$\sigma \mathbf{A} \mathbf{X} = \mathbf{B} \mathbf{X}, \quad (7)$$

where  $\mathbf{A}$  and  $\mathbf{B}$  are all  $(N-1) \times (N-1)$  real matrices, and represent the discretization of the differential operators. When  $\sigma$  is a complex number, instability will

occur. Its real part denotes the unstable perturbation propagation frequency, and the imaginary part the unstable growth rate.  $\mathbf{X} = (\Psi_2, \Psi_3, \Psi_4, \dots, \Psi_N)^T$  is the eigen function corresponding to  $\sigma$ , i.e., spectrum function, which gives the value of stream function at each grid point. Equation (7) is solved by using Matlab 7.0 with latest upgrades.

### 2.2 The barotropic primitive equation vortex model

The linearized barotropic primitive equations in a cylindrical coordinate are

$$\begin{cases} \frac{\partial U}{\partial t} + \bar{\Omega} \frac{\partial U}{\partial \lambda} - \tilde{f}V = -C_0^2 \frac{\partial \Phi}{\partial r}, \\ \frac{\partial V}{\partial t} + \bar{\Omega} \frac{\partial V}{\partial \lambda} + \hat{f}U = -C_0^2 \frac{\partial \Phi}{r \partial \lambda}, \\ \frac{\partial \Phi}{\partial t} + \bar{\Omega} \frac{\partial \Phi}{\partial \lambda} + \left( \frac{\partial r U}{r \partial \lambda} \right) = 0, \end{cases} \quad (8)$$

where  $C_0^2 = \bar{\phi}$ ,  $U = C_0^2 u$ ,  $V = C_0^2 v$ ;  $\tilde{f} = f + 2\bar{V}/r = f + 2\bar{\Omega}$  is the modified Coriolis parameter;  $\hat{f} = f + \bar{\Omega} + d\bar{V}/dr$  is the absolute vorticity;  $u, v$ , and  $\phi$  are perturbation radial, tangential winds, and surface-height perturbation, respectively;  $\bar{\phi}$  is a constant resting geopotential height. Here,  $\bar{V}$  also satisfies the gradient wind balance. The boundary condition of this model is

$$r = 0, U = 0; \quad r = \tilde{r}, U = 0. \quad (9)$$

The solution to Eq. (8) can be set as

$$\begin{bmatrix} U \\ V \\ \Phi \end{bmatrix} = \begin{bmatrix} i\hat{U}(r) \\ \hat{V}(r) \\ \hat{\phi}(r) \end{bmatrix} e^{i(n\lambda - \sigma t)}. \quad (10)$$

An ordinary differential equation set can be obtained after substituting Eq. (10) into Eq. (8) and omitting “ $\wedge$ ” on  $\hat{U}$ ,  $\hat{V}$ , and  $\hat{\phi}$ ,

$$\begin{cases} n\bar{\Omega}U + \tilde{f}V - C_0^2 \frac{d\phi}{dr} = \sigma U, \\ \hat{f}U + n\bar{\Omega}V + \frac{C_0^2}{r} n\phi = \sigma V, \\ \frac{drU}{r dr} + \frac{n}{r} V + n\bar{\Omega}\phi = \sigma \phi. \end{cases} \quad (11)$$

A generalized matrix-eigenvalue problem can also be obtained after discretizing Eq. (11) with the consideration of the boundary condition in Eq. (9) (Huang and Zhang, 2003).

### 3. Definition of the basic flow

An empirical expression is often used to define the radial change of tangential velocity when a TC-like vortex is studied. The vortex studied here is constructed by smoothly connecting piecewise constant vorticity profiles, with relatively low vorticity in the eye, very high vorticity in the eyewall annulus, and then very low vorticity in the far field (Nolan and Montgomery, 2002). Its formula is

$$\bar{\zeta}(r) = \begin{cases} \zeta_1, & 0 \leq r \leq r_1 - d_1; \\ \zeta_1 S[(r - r_1 + d_1)/2d_1] + \zeta_2 S[(r_1 + d_1 - r)/2d_1], & r_1 - d_1 \leq r \leq r_1 + d_1; \\ \zeta_2, & r_1 + d_1 \leq r \leq r_2 - d_2; \\ \zeta_2 S[(r - r_2 + d_2)/2d_2] + \zeta_3 S[(r_2 + d_2 - r)/2d_2], & r_2 - d_2 \leq r \leq r_2 + d_2; \\ \zeta_3, & r_2 + d_2 \leq r \leq r_3 - d_3; \\ \zeta_3 S[(r - r_3 + d_3)/2d_3], & r_3 - d_3 \leq r \leq r_3 + d_3; \\ 0, & r_3 + d_3 \leq r < \infty. \end{cases} \quad (12)$$

Here,  $\bar{\zeta}$  is basic-state relative vorticity;  $S(x) = 1 - 3x^2 + 2x^3$  is the cubic Hermitian polynomial that satisfies  $S(0) = 1$ ,  $S(1) = 0$ , and  $S'(0) = S'(1) = 0$ . Values for  $D_i, r_i$ , and  $\zeta_i$  ( $i=1, 2, 3$ ) are also given by Nolan and Montgomery (2002). The absolute vorticity (hereafter referred to as vorticity for short) and velocity profiles of this vortex are shown in Fig. 1. The vortex has a maximum wind speed near the radius of about 34.5 km from the TC center. The vorticity of the vortex reaches its maximum at the radius of about 26 km from the TC center, which can be called the radius of maximum vorticity (RMV). The vorticity gradient is relatively large between 15 and 40 km from the TC center.

### 4. Results and discussion

A previous theoretical analysis shows that, in models 1 and 2, the appointed basic-state profiles satisfy the necessary instability conditions (Huang, 2006). The barotropic instability condition is satisfied in Model 1, and so is the barotropic and super-high

speed instability condition in Model 2.

Using the basic-state profile and vortex models described above, we computed the eigenvalues and eigenvectors of the coefficient matrix for each wavenumber considered. Computational results show that the basic-state flow may be disturbed for some wavenumbers when instability criteria are satisfied, which is consistent with the theoretical deduction. The growth rates of the most unstable modes in both models are shown in Fig. 2. The vortex is most unstable for  $n = 3$  in both models, so azimuthal wavenumbers are all taken as 3 when the computation results are analyzed. In the two models, a couple of unstable perturbations coexist, one of which is growing and the other is decaying. We will only discuss the growing unstable mode in the following text.

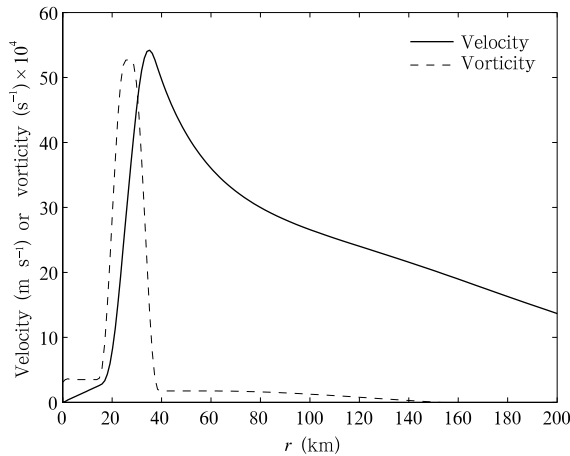


**Fig. 1.** Absolute vorticity (solid) and tangential velocity (dashed) for the basic-state vortices.

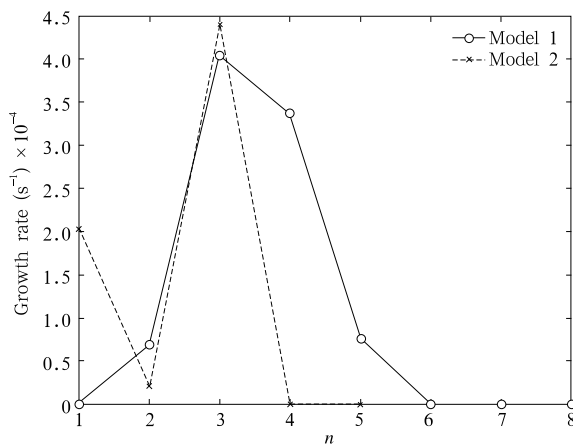


**Fig. 2.** The stability diagram for the vortex as a function of azimuthal wavenumber.

The perturbation stream function and absolute vorticity of the most unstable mode of Model 1 are shown in Fig. 3. From this figure, we can deduce some properties of the mode. From the vorticity field, we can see that the mode is made up of two concentric sets of perturbations that lie on either side of the basic-state vorticity maximum (also where the vorticity gradient changes sign). The maximum stream function appears at RMW and RMV, respectively. A spiral band-like structure can be seen. Perturbation decays fast outside the RMW, and exhibits no wave-like structure along the radial direction. The RMV is closely associated with annulus of intense precipitation known as the eyewall, and it resides in the interior of the RMW. The spiral band-like structure can not be seen even very far from the center.

In another word, Model 1 only shows an unstable eyewall-like structure and an inner spiral-band structure of this vortex. This unstable mode can be interpreted as an unstable discrete VRW propagating relative to the basic-state flow. It extracts energy from the vortex mainly through barotropic energy conservation (Huang, 2006). Its propagation stops at the radius of about 140 km from the TC center where absolute vorticity of the basic-state flow vanishes. So there arises a question as to whether the barotropic nondivergent model can explain the dynamical properties of the unstable inner and outer spiral bands of a TC at the same time.

The unstable perturbation in Model 2 (Fig. 4) is different in structure from that in Model 1 (Fig. 3). The distributions of the perturbation vorticity are analogous to the schematic rendering of the traditional coupled VR (vortex-Rossby) wave-type barotropic instability and the IB (inertia-buoyancy) wave coupled to a VR wave-type barotropic instability, respectively, as shown in Hodyss and Nolan (2008). The unstable perturbation reveals a spiral band-like structure outside the RMW, which rotates cyclonically outward in the whole region of this vortex. The bands are narrow and long. In this model, the unstable perturbation is divided into three parts: eyewall (the perturbation maximum inside the RMW), inner spiral band at radii smaller than 140 km, and outer spiral band at radii larger than 140 km.

We computed the radial distribution of the relative vorticity and divergence of the unstable perturbation (at  $\lambda = 0$ ) to analyze its dynamic properties (Fig. 5). It can be seen that the vorticity almost vanishes outside the RMW. However, the divergence shows positive or negative values alternately within the whole vortex. In order to compare the relative magnitude of its divergence and vorticity, a divergent-vorticity ratio (referred to as D-V ratio hereafter),  $\mu$ , is computed

using the formula

$$\mu(r_i) = \frac{|D(r_i)|}{|\zeta(r_i)|}, \quad (13)$$

where  $D$  and  $\zeta$  denote the divergence and relative vorticity at a certain radius  $r_i$ . The ratio denotes the relative importance between divergent and vertical motions. The divergence dominates when  $\mu$  is larger than 10 and so does the vortex motion when it is less than

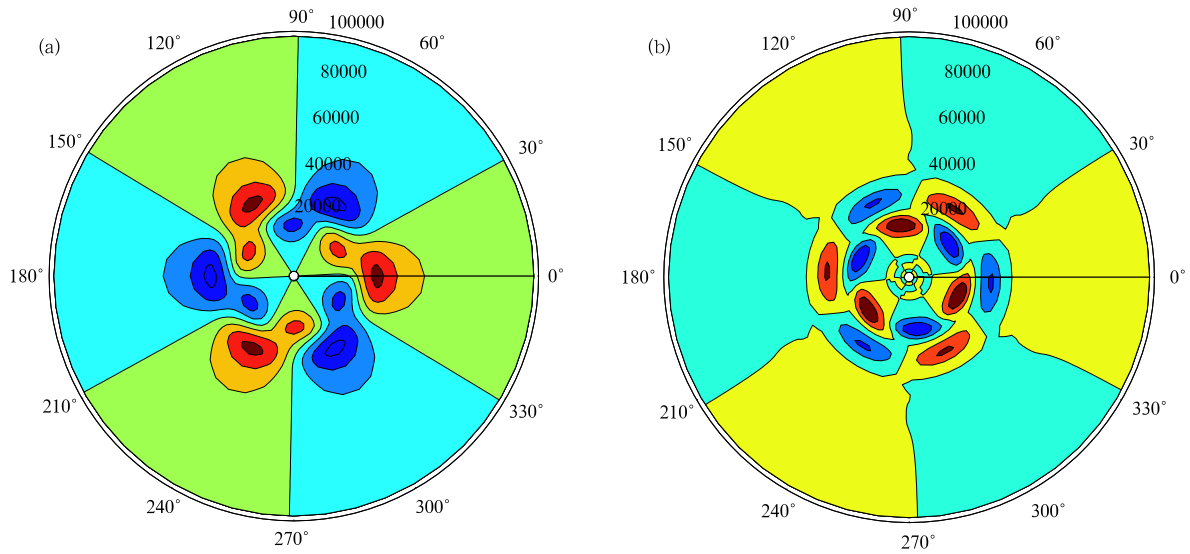


**Fig. 3.** Stream function (a;  $m^2 s^{-1}$ ) and vorticity (b;  $s^{-1}$ ) of the unstable perturbation in Model 1 inside a radius of 100 km from the TC center.

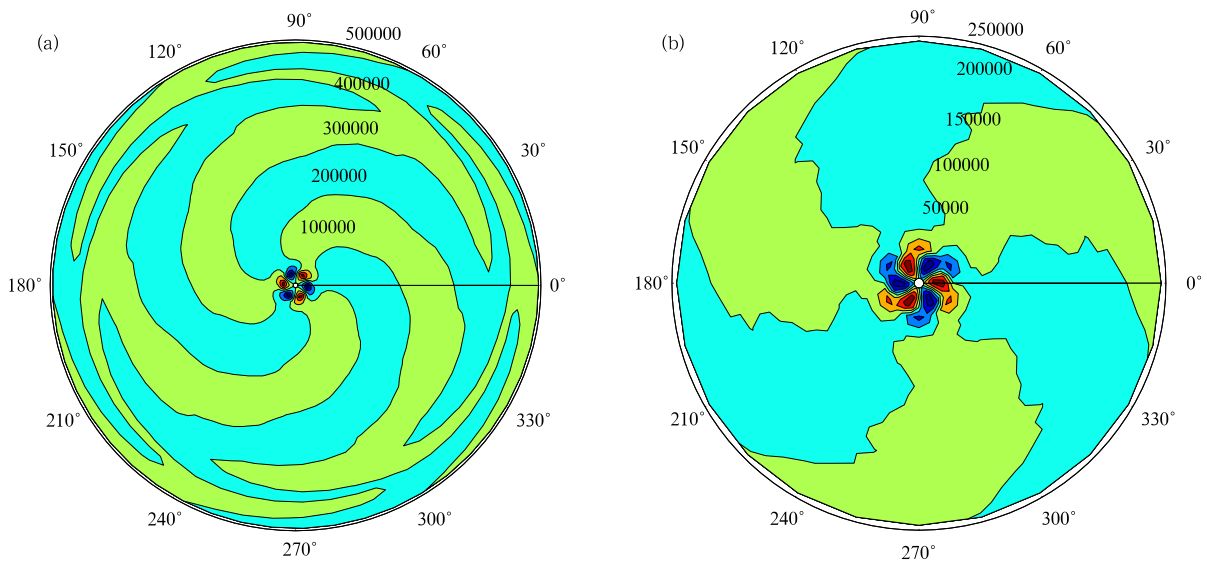


**Fig. 4.** Geopotential height (a; gpm) and vorticity (b;  $s^{-1}$ ) for  $r < 250$  km of the unstable perturbation in Model 2.

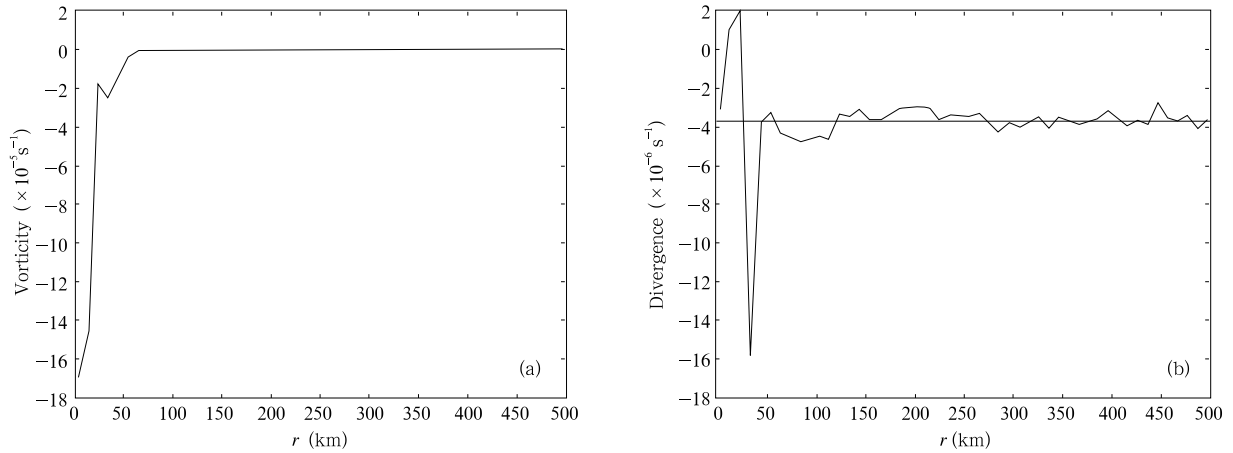


**Fig. 5.** Radial distributions of relative vorticity (a) and divergence (b) of the unstable perturbation in Model 2.

0.1. It can be seen from Fig. 6 that the ratio values are very small at the radii between the RMV and RMW where the perturbation maximum appears. The values increase gradually 100 km away from the vortex center and reach a peak near  $r = 450$  km.

The effect of the rotation of the basic-state flow vanishes near the stagnation radius ( $r = 140$  km) of the VRW. However, divergent motion still works outside this radius. Therefore, the formation of the outer spiral bands shall be closely related to divergence.

The spectrum-function distribution of the most unstable perturbation in Model 2 is shown in Fig. 7. The distributions of  $\phi$  and  $U$  (see Eq. 8) at the RMV

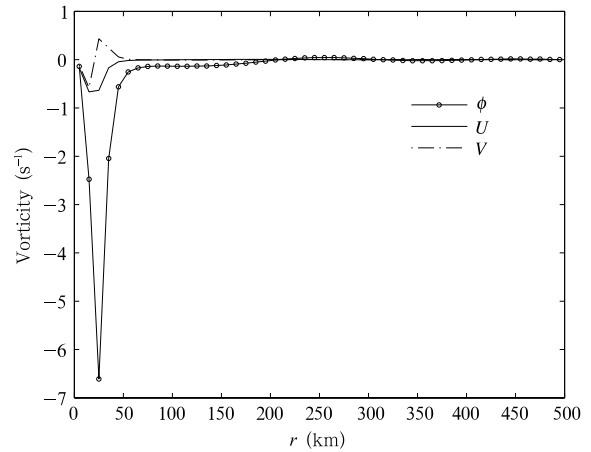


**Fig. 7.** Spectrum-function distributions of the most unstable perturbation in Model 2. The solid line denotes  $U$  ( $\text{m s}^{-1}$ ); the dashed line  $V$  ( $\text{m s}^{-1}$ ); and the dot dashed line  $\phi$  ( $10^{-3}$  gpm).

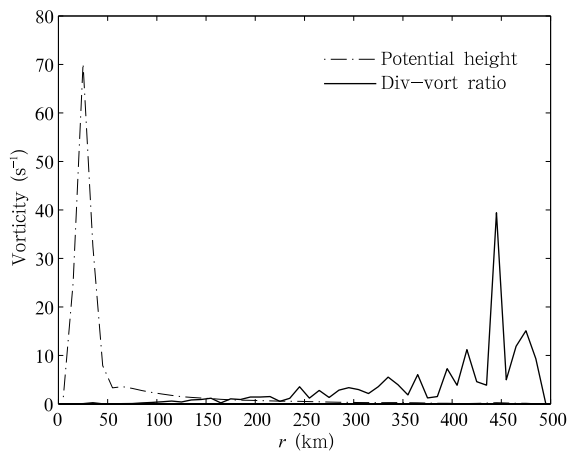


**Fig. 6.** Radial distributions of geopotential height (dashed;  $10^{-4}$  gpm) and divergence-vorticity ratio (solid) of the most unstable perturbation in Model 2. The horizontal axis is radius.

are similar to those at the RMW, when the D-V ratio is much smaller than 1, suggesting that the perturbation is quasi-balanced within this region. They are apparently different outside this region, indicating that the perturbation is unbalanced there. As is well known, the vortex wave is quasi-balanced and the inertia-gravitational wave is unbalanced, so this perturbation shall not be a pure VRW or inertia-gravitational wave. It shall be interpreted as a mixed vortex Rossby – inertia gravitational wave, which possesses the properties of the first or second kind of wave at different radii. The VRW is dominant where a large perturbation appears. The wave spectrums of this model using the same basic-state

flow as in Huang (2006) were computed as well. Continuous spectrums of the inertia-gravitational and vortex-Rossby wave overlap each other, which also validate the conclusion mentioned above.

## 5. Summary

A barotropic nondivergent vortex model (Model 1) and a barotropic primitive equation vortex model (Model 2) are used respectively to study the dynamical instability of waves in a TC-like vortex. In Model 1, the inertia-gravitational wave is filtered, and the VRW is ageostrophic because of its relative small space scale. However, they are quasi-balanced. In Model 2, the maximum wind speed of the symmetric TC-like basic flow is very large, but its space scale is relative small, so the continuous spectrum regions of the inertial-gravitational wave and the VRW overlap each other. The waves in this overlapping region cannot be distinguished as slow or fast waves from their frequency. The integral of these wave modes can be interpreted as a mixed vortex Rossby – inertial gravitational wave packet. The instability in this wave packet shall be explained as unbalanced instability (Huang, 2006).

We may view the unstable mode in Model 2 as having three parts, i.e., eyewall, inner and outer spiral bands. The eyewall part exhibits properties of a VRW. It peaks approximately where  $|d\bar{\eta}/dr|$  is maximum. The eigenmode shows a spiral band-like structure that propagates away from the vortex outside the RMW. As the radius  $r$  increases, the mean cyclonic flow becomes negligible. So in its outer spiral band part, the eigenmode also displays a spiral band-like structure that propagates away from the vortex. There is no vorticity gradient to support this propagation. Therefore, the outer part of this mode possesses properties of an inertial-gravitational wave. The property of the mixed wave is most evident in the inner spiral band part. We can conclude that the unbalanced property of the wave outside the stagnation radius of the VRW is one of the important reasons for the formation of the outer spiral band in TCs.

In a word, the discrete modal instability of the pure VRW can account for the generation of the eye-

wall and the inner spiral band, but cannot directly account for the generation of the outer spiral band. Divergence plays an important role in the formation of the outer spiral band. So only the instability of the mixed wave can interpret the generation of the eyewall, the inner and outer spiral bands at the same time. This conclusion is different from a previous statement that says the inner and outer spiral bands shall be explained with different mechanisms (Guinn and Schubert, 1993). In this paper, we find that an unstable mixed wave mode can explain the generation and structure of both the inner and the outer spiral bands simultaneously.

This study sheds light on the instability property of spiral bands in TCs. However, only barotropic vortex modes are examined here, without considering the effect of the baroclinic and thermodynamic processes. A more comprehensive study on the instability of spiral bands in TCs shall be carried out in the future.

## REFERENCES

- Abdullah, A. J., 1966: The spiral bands of a hurricane: A possible dynamics explanation. *J. Atmos. Sci.*, **23**, 367–375.
- Avila, L. A., 1998: Forecasting tropical cyclone intensity changes: An operational challenge. Preprints, Symposium on Tropical Cyclone Intensity Change. Amer. Meteor. Soc., Phoenix, Arizona, 11–16.
- Chanh, Q. Kieu, 2004: Analytical theory for the early stage of the development of hurricanes. Part I. <http://arxiv.org/abs/physics/0407073>.
- Chen Lianshou, 2001: An overview on progress in research on tropical cyclone motion. National workshop on tropical cyclones. China Meteorological Press, Beijing, 1–9. (in Chinese)
- Chen Yingyi, 1984: Conservation of wave action and evolution in the eddy. *Science in China (Ser. B)*, **27**(10), 1059–1068.
- Chow, K. C., K. L. Chen, and K. H. L. Alexis, 2002: Generation of moving spiral bands in tropical cyclones. *J. Atmos. Sci.*, **59**, 2930–2950.
- DeMaria, M., and J. Kaplan, 1999: An updated statistical hurricane intensity prediction scheme for the Atlantic and eastern North Pacific basins. *Wea. Forecasting*, **14**, 326–337.

- Duan Yihong, Yu Hui, and Wu Rongsheng, 2005: Review of the research in the intensity change of tropical cyclone. *Acta Meteor. Sinica*, **63**(5), 636–642. (in Chinese)
- Guinn, T. A., and W. H. Schubert, 1993: Hurricane spiral bands. *J. Atmos. Sci.*, **50**, 3380–3403.
- Hodyss, D., and D. S. Nolan, 2008: The Rossby-inertia-buoyancy instability in baroclinic vortices. *Phys. Fluids*, **20**, 096602-096621.
- Huang Hong, 2006: A study on perturbations in tropical cyclone-scale vortex. Ph. D. dissertation. PLA University of Science and Technology, 273 pp. (in Chinese)
- Huang Hong and Zhang Ming, 2003: Study on destabilization of spiral wave in barotropic vortex. *Chinese J. Tropical Meteor.*, **19**(2), 197–202. (in Chinese)
- Huang Ruixin and Chao Jiping, 1980: The linear theory of spiral cloud bands of typhoon. *Chinese J. Atmos. Sci.*, **4**(2), 148–158. (in Chinese)
- Liu Shikuo, 1981: Inertia-gravitational wave in typhoon. Conference on Typhoon. Shanghai, 180–189.
- Liu Shikuo and Yang Dasheng, 1980: The spiral structure of typhoon. *Acta Meteor. Sinica*, **38**(3), 193–205. (in Chinese)
- Macdonald, N. J., 1968: The evidence for the existence of Rossby-like waves in the hurricane vortex. *Tellus*, **20**, 138–150.
- Maynard, R. H., 1945: Radar and weather. *J. Meteor.*, **2**, 214–226.
- McAdie, C., and M. B. Lawrence, 2000: Improvements in tropical cyclone track forecasting in the Atlantic basin in 1970–1998. *Bull. Amer. Meteor. Soc.*, **81**, 989–998.
- Montgomery, M. T., and R. J. Kallenbach, 1997: A theory for vortex Rossby-waves and its application to spiral bands and intensity changes in hurricanes. *Quart. J. Roy. Meteor. Soc.*, **123**, 435–465.
- Nolan, D. S., and M. T. Montgomery, 2002: Nonhydrostatic, three-dimensional perturbations to balanced, hurricane-like vortices. Part I: Linearized formulation, stability, and evolution. *J. Atmos. Sci.*, **59**, 2989–3020.
- Shapiro, L. J., and M. T. Montgomery, 1993: A three-dimensional balance theory for rapidly rotating vortices. *J. Atmos. Sci.*, **50**, 3322–3335.
- Wang, Y., 2001: An explicit simulation of tropical cyclones with a triply nested movable mesh primitive equation model: TCM3. Part I: Model description and control experiment. *Mon. Wea. Rev.*, **129**, 1370–1394.
- Wang, Y., 2002a: Vortex Rossby waves in a numerically simulated tropical cyclone. Part I: Overall structure, potential vorticity and kinetic energy budgets. *J. Atmos. Sci.*, **59**, 1213–1238.
- Wang, Y., 2002b: Vortex Rossby waves in a numerically simulated tropical cyclone. Part II: The role in tropical cyclone structure and intensity change. *J. Atmos. Sci.*, **59**, 1239–1262.
- Wexler, H., 1947: Structure of hurricanes as determined by radar. *Ann. N. Y. Acad. Sci.*, **48**, 821–844.
- Willoughby, H. E., H. -L. Jin, S. J. Lord, et. al., 1984: Hurricane structure and evolution as simulated by an axisymmetric, nonhydrostatic numerical model. *J. Atmos. Sci.*, **41**, 1169–1186.
- Xu Xiangde, 1999: Comprehensive dynamic model of tropical cyclone anomalous motion track. 11th National Workshop on Tropical Cyclones. Meteorological Research Institute, Beijing, 15–17. (in Chinese)
- Yu Zhihao, 2002: The spiral rain bands of tropical cyclone and vortex rossby waves. *Acta Meteor. Sinica*, **60**(4), 502–507. (in Chinese)
- Zeng Qingcun, Li Rongfeng, and Zhang Ming, 1990: Spectra and spectral functions of rotating two dimensional compressive motion. Part I: Distribution of spectrum points. *Chinese J. Atmos. Sci.*, **14**(2), 129–142. (in Chinese)
- Zeng Qingcun, Li Rongfeng, and Zhang Ming, 1991: Spectra and spectral functions of rotating two dimensional compressive motion. Part II: Structure of spectral functions and further discussion on spectra. *Chinese J. Atmos. Sci.*, **15**(1), 1–15. (in Chinese)
- Zhang Ming, 1995: A study of the instability in the barotropic vortex. *Chinese J. Atmos. Sci.*, **19**(6), 677–686. (in Chinese)
- Zhang Ming and Zeng Qingcun, 1983: Preliminary numerical simulation results of spiral bands in typhoon. Conference on Typhoon. Shanghai Science & Technology Press, Shanghai, 92–100. (in Chinese)